Surface Modification of Hexatriacontane: A Comparison Between Exposure to An Electron-Assisted CF*n Radical Flux and to a Microwave Low-Pressure CF4 Plasma

Fabienne Poncin-Epaillard[a]; Isabelle Rouger[bc]; Jean-Paul Gilles[b]; Jean-Paul Grandchamp[b]

[a] Laboratoire de Chimie et Physicochimie Macromoléculaire, URA au CNRS 509, Université du Maine, Le Mans Cedex, France [b] Institut d'Electronique Fondamentale, URA au CNRS 22, Université Paris XI, Orsay Cedex, France [c] Laboratoire des Réacteurs Chimiques en Phase Plasma, ENSCPUPMC, Paris Cedex, France

PLEASE SCROLL DOWN FOR ARTICLE

SURFACE MODIFICATION OF HEXATRIACONTANE: A COMPARISON BETWEEN EXPOSURE TO AN ELECTRON-ASSISTED CF$_n^*$ RADICAL FLUX AND TO A MICROWAVE LOW-PRESSURE CF$_4$ PLASMA

FABIENNE PONCIN-EPAILLARD*

Laboratoire de Chimie et Physicochimie Macromoléculaire
URA au CNRS 509, Université du Maine
Avenue Olivier Messiaen, 72017 Le Mans Cedex, France

ISABELLE ROUGER,† JEAN-PAUL GILLES, and
JEAN-PAUL GRANDCHAMP

Institut d'Electronique Fondamentale
URA au CNRS 22, Université Paris XI
Bât 220, 91405 Orsay Cedex, France

ABSTRACT

Surface modification of hexatriacontane in a fluorocarbon plasma environment has been studied. Hexatriacontane, a C$_{36}$ n-alkane deposited on Al foils, has been chosen as a model molecule to simulate high density polyethylene. In order to get more insight on the relevant mechanisms, the samples were first exposed to a flux of CF$_n^*$ radicals either alone or in synergy with low-energy electrons, and second to CF$_4$ low-pressure microwave plasma. The surface modifications were studied by contact angle measurement, Fourier transmission infrared spectroscopy, and electronic spectroscopy for chemical analysis. The CF$_n^*$ radical exposure induces CF$_n$ and F chemisorption; electron-assisted exposure to radicals

†Present address: Laboratoire des Réacteurs Chimiques en Phase Plasma, ENSCP-UPMC, 11 rue P. et M. Curie, 75231 Paris Cedex 05, France.

induces the grafting of CF, CF_2, and CF_3 groups on the CH_2 groups of the molecule, and the microwave plasma exposure entails the formation of a large amount of CF and CF_2 groups.

INTRODUCTION

Polymer surface modification by low-pressure plasma has been widely described [1–6]. It depends on both plasma excitation and on the nature of the polymer. Only a few attempts have been made to compare the efficiency of different plasma excitations on polymer modifications [7–9]. Some authors have reported on the effects of CF_4 microwave (433 MHz) plasma on a polymer surface [10, 11].

Some attempts involved setting up a surface model [12–15]. Polyolefins and their model molecules, some n-alkanes, have been modified by tetrafluoromethane microwave plasma [10, 15]. The molecules chosen are high-density polyethylene (HDPE) and hexatriacontane (HTC), low-density polyethylene (LDPE) and paraffin, polycaprolactone (PCL), and octadecyl octadecanoate (ODO). It has been found, except for paraffin, that model surfaces have the same behavior as the corresponding polymers. The chemical structures of most polyolefins or polyesters fluorinated by cold plasma present a similar composition: a Teflon-like one with CF_2 groups prevalent. Plasma modification was also described as the sum of two mechanisms: degradation and fluorination. But in such a plasma, the surface is simultaneously bombarded by molecules, radicals, ions, electrons, and photons. The specific features of each flux are not well known. A specific plasma source has been developed for operation with CF_4 [16–18] to deliver the plasma-selected species downstream: 1) a flux of radicals (and photons) when both ions and electrons are trapped within the plasma chamber, 2) radicals + electrons if the ions are trapped, or 3) radicals + ions if the electrons are trapped. Illustrations are the reactive ion beam etching process (RIBE) used to achieve SiO_2/Si selective and anisotropic etching, and the electron-assisted polymerization of CF_x radicals process [19, 20]. The samples were treated for various periods of time and seven main exposure conditions, as summarized in Table 1. These effects have been studied and compared.

TABLE 1. Summary of the Different Treatment Conditions

Case	Impinging particles	Plasma operation[a]	Main interactive particles
A	CF_n^* radicals	Maxi-ERIS/high pressure	CF_3
B	CF_n^* radicals + e	Maxi-ERIS/high pressure	CF_3
C	CF_n^* radicals	Maxi-ERIS/low pressure	CF_2 and CF
D	CF_n^* radicals + e	Maxi-ERIS/low pressure	CF_2 and CF
E	CF_n^* radicals + ions + e	MWP	CF, CF_2, and CF_3
F	CF_n^* radicals + ions + e	Remote MWP ($z = -5$ cm)	CF, CF_2, and CF_3
G	CF_n^* radicals + ions + e	Remote MWP ($z = -30$ cm)	CF, CF_2, and CF_3

[a]z = distance between edge of plasma and substrate.

EXPERIMENTAL PART

Plasma and Maxi-ERIS Equipment

Microwave plasma (MWP) equipment (Fig. 1a), processes of plasma treatment have been previously described [21–23]. The experiments were all run in the same conditions: incident power (P_i) = 63 W, reflected power (P_r) < 10^{-2} W, CF$_4$ flow (D) = 30 sccm, pressure (p) = 0.35 mbar. Only two parameters were variable: treatment time t (seconds) and sample position in the reactor z (cm). If $z = 0$, the substrate is at the edge of the visible part of the plasma; if $z > 0$, the sample is treated in the discharge; and $z < 0$ means a postdischarge treatment.

A specific dc discharge, the Maxi-electrostatic reflex ion source (Maxi-ERIS), has been developed for operation with fluorocarbon gases at low pressure without lifetime problems and with reduced contamination [18]. The operation pressure (P_s) range within the source chamber is from 1×10^{-4} mbar up to 20×10^{-4} mbar. This pressure is recorded by a capacitance manometer. As shown schematically in Fig. 1(b), it is a three-electrode structure with a hot tantalum cathode and a small graphite anode, both located within the cylindrical discharge chamber. The latter is negatively biased with respect to the hot cathode, and thereby ensures the electrostatic containment (reflex effect) of the primary ionizing electrons that are initially accelerated by the dc discharge voltage (V_D) applied between the anode and the cathode. The extraction optics is a three-grid system constructed of graphite. This system permits an electrostatic selection of the particles that impinge on the target located 13 cm downstream of the source. When an ion beam is required, this structure delivers a 7-cm diameter ion beam in the downstream interaction chamber pumped by a nitrogen-trapped diffusion pump (700 L/s for argon). The pressure in the interaction chamber (p_E), recorded by both a capacitance manometer and a Penning ionization gauge, is an order of magnitude lower than P_s. When both ions and electrons are trapped within the plasma chamber, only neutral species (radicals, molecules, and photons) effuse toward the target. For high pressure in the interaction chamber (10^{-4} mbar), directional neutral species flux at the target was evaluated as 3×10^{16} cm$^{-2}\cdot$s^{-1}, and can be compared to the isotropic flux corresponding to the local pressure: 10^{16} cm$^{-2}\cdot$s^{-1}. An electron beam could effuse simultaneously with reactive neutral species from Maxi-ERIS. According to the discharge model [16, 17], two electron populations exist: plasma electrons and primary electrons, partially trapped in the discharge structure with an initial energy equal to eV_D. In our experimental conditions, plasma potential is close to the target potential, and only the latter species can reach the target. Their energy, W_e, is determined both by the potential V_D and the unknown value x corresponding to the loss of energy due to ionizing or exciting collisions with any gas particle in the discharge chamber. As a first approximation, the extracted electrons are assumed to come directly from the cathode, so $W_e = e(V_D + x) \approx eV_D$. The samples to be exposed to the plasma are introduced into the interaction chamber through a load-lock system. They are clamped onto an electrically insulated and water-cooled copper target. The target is driven in and out of the interaction chamber by a motor system. Samples are exposed at normal incidence, whatever the experimental conditions. A Faraday cup is included within the target to monitor the electron current density which was measured as 0.12 mA$\cdot$cm^{-2}.
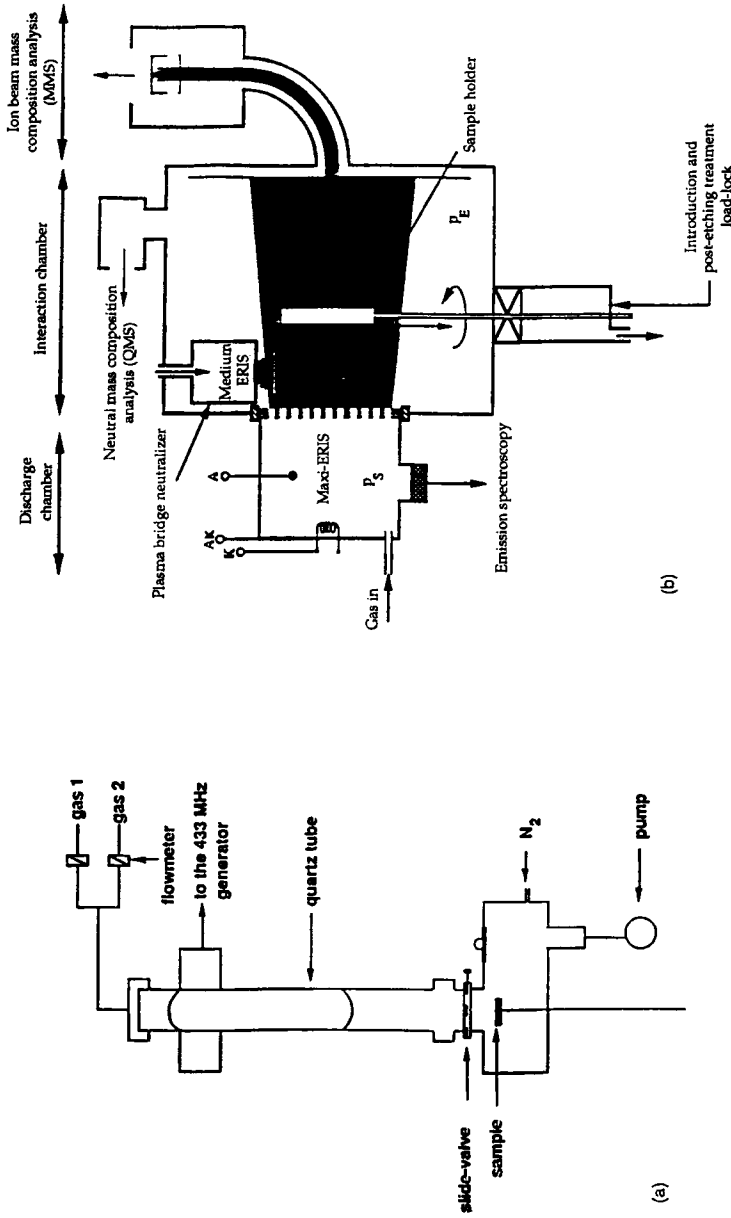
FIG. 1.   Experimental set-up of (a) MWP and (b) Maxi-Eris for sample exposure downstream for a dc-excited CF_4 plasma. K, hot cathode; A, anode; AK, electron-reflecting anticathode.

Emission spectroscopy was performed with a monochromator Jobin Yvon HR 320 having a focal length of 32 cm equipped with a 1200 grooves/mm grating. The photons were detected with a Hamamatsu R928 photomultiplier whose spectral response ranges from 185 to 930 nm. The output signal was amplified by a Spectralinke (Jobin Yvon) connected to a chart recorder. The emission light was analyzed at the edge of the microwave plasma or in the Maxi-ERIS source.

Mass spectroscopy was performed on Maxi-ERIS equipment. The ion beam composition was on-line recorded with a magnetic-mass-spectrometer (MMS); the composition of the stable neutrals present within the interaction chamber were recorded with a quadrupole mass spectrometer (QMS) located within a differentially pumped chamber. Ion beam composition spectroscopy was used as a complementary diagnostic of the discharge. However, ions are trapped in the discharge chamber during sample treatment. Because of the dc excitation (80–130 eV) of the hot cathode discharge linked to efficient electrostatic containment, the primary electrons have very large dissociation and ionization yields. Therefore, the injected neutrals may be extensively fragmented as CF_x radicals. The fragmentation is more extensive as the discharge voltage and current discharge increase, and as the injected neutral flow decreases.

Surface Preparation

Hexatriacontane (Aldrich), recrystallized from *n*-hexane (spectroscopic grade, Aldrich) was spread on an aluminum sheet heated to its melting point with a Conway stick, leading to a film 6 μm thick. The Al substrate had been cleaned prior to heating with a sulfochromic acid solution and washed several times with distilled water and ethanol. The films were slowly cooled and kept under vacuum.

All the films had a fixed area: 15 cm^2 in microwave plasma, 8 cm^2 for the Maxi-ERIS source, and a constant thickness of 6 μm. The film is characterized described elsewhere [24].

The CF_4 gas (Matheson or Air liquide) had a purity of 99.995%.

Surface Analyses

The SEM photographs were made on a Hitachi 52300 in the Département de Génie Mécanique, Institut Universitaire de Technologie, Université du Maine (Le Mans, France).

The FT-IR spectra were recorded on a FT-IR Perkin Elmer 1750, with a microcomputer 7700, attenuated total reflection (ATR, 200 scans, Θ between 30 and 60°).

The electronic spectroscopy for chemical analysis (ESCA) was developed by the Laboratoire de Physique des Couches Minces, Université de Nantes (Nantes, France). The instrument was calibrated to the Au reference.

The surface energies of the samples were calculated from the contact angles of distilled water, glycerol, and diiodomethane (volume: 4 μL) and from the Dupré relation [25] as described in Reference 1. The measurement error is less than 5°. Surface energies of different liquids were as follows:

$$\gamma_{H_2O} = 72.75 \, mJ \cdot m^{-2}, \; \gamma_{H_2O}^{D} = 21.75 \, mJ \cdot m^{-2}, \; \gamma_{H_2O}^{P} = 51.0 \, mJ \cdot m^{-2}$$

$$\gamma_{i2} = 50.8\,\text{mJ}\cdot\text{m}^{-2}, \; \gamma_{i2}^D = 49.5\,\text{mJ}\cdot\text{m}^{-2}, \; \gamma_{i2}^P = 1.3\,\text{mJ}\cdot\text{m}^{-2}$$

$$\gamma_{gly} = 63.4\,\text{mJ}\cdot\text{m}^{-2}, \; \gamma_{gly}^D = 37.0\,\text{mJ}\cdot\text{m}^{-2}, \; \gamma_{gly}^P = 26.4\,\text{mJ}\cdot\text{m}^{-2}$$

Five measurements with each liquid were made on every sample.

RESULTS AND DISCUSSION

Nature of Reactive Fluorinated Species

Optical Spectroscopy of Microwave CF_4 Plasma Emission (Fig. 2a)

Main bands or lines observed (Fig. 2a) correspond to fluorinated species $CF^{\circ}*$ (221 nm), $CF_2^{+}*$ (continuum), and $CF_2^{\circ}*$ (between 257 and 330 nm). F* emission at 623 nm is detected, but its emission at 703.7 nm is not detected, probably due to a bad response of this grating near 700 nm. This microwave plasma seems to lead to the same optical spectrum as for RF/CF_4 plasmas [26–28]. While the $CF_3^{\circ}*$ radical leads to a continuum centered at 614 nm that is noticed in the corona discharge [29], no band or continuum is detected here, and $CF_3^{\circ}*$ should not exist in this kind of plasma.

Optical Spectroscopy of CF_4 Maxi-ERIS Emission (Figs. 2b and 2c)

Here, optical spectroscopy does not show evidence of $CF^{\circ}*$, $CF_2^{\circ}*$, or $CF_3^{\circ}*$ radicals. $CF_2^{+}*$ (continuum) emissions are detected and, as for MWP experiment, fluorine atom emission at 623 nm is noticed. No simple dependence of $CF_2^{+}*$ continuum on CF_4 flux is pointed out, because CF_4 fragmentation varies with pressure. Some impurities [CN (388.3, 401.1 nm), C_2 (409.3, 435.3, 473.6 nm), and H (434.0, 486.1 nm)] are detected.

Mass Spectrometry of CF_4 Maxi-ERIS

The composition of stable neutrals (Figs. 3a and 3c) within the interaction chamber and ions (Figs. 3b and 3d) illustrates the dependence of CF_4 fragmentation on pressure: the lower the pressure, the higher the fragmentation. Without discharge, the neutral spectrum shows only the CF_3^+ parent peak of the CF_4 molecule. The spectra of the neutral phase (Figs. 3a and 3c) clearly show that heavy fluorocarbon molecules such as C_2F_n and C_4F_n are also synthesized. The existence of these species may be due to the presence of a large amount of unsaturated radicals such as CF_2 both within the source chamber and the ion beam chamber. Even if the excited fluorinated species in plasma phase seem to be different than those in CF_4 MWP equipment, Maxi-ERIS could be used as a MWP model because fluorinated species selectivity could be achieved.

Surface Modification of Hexatriacontane: Kinetic Aspects—Dependence on Irradiation Time

Cold plasma modification of organic material can be explained in terms of functionalization, of fluorination when tetrafluoromethane is used, and of degradation [30]. The kinetics are based:
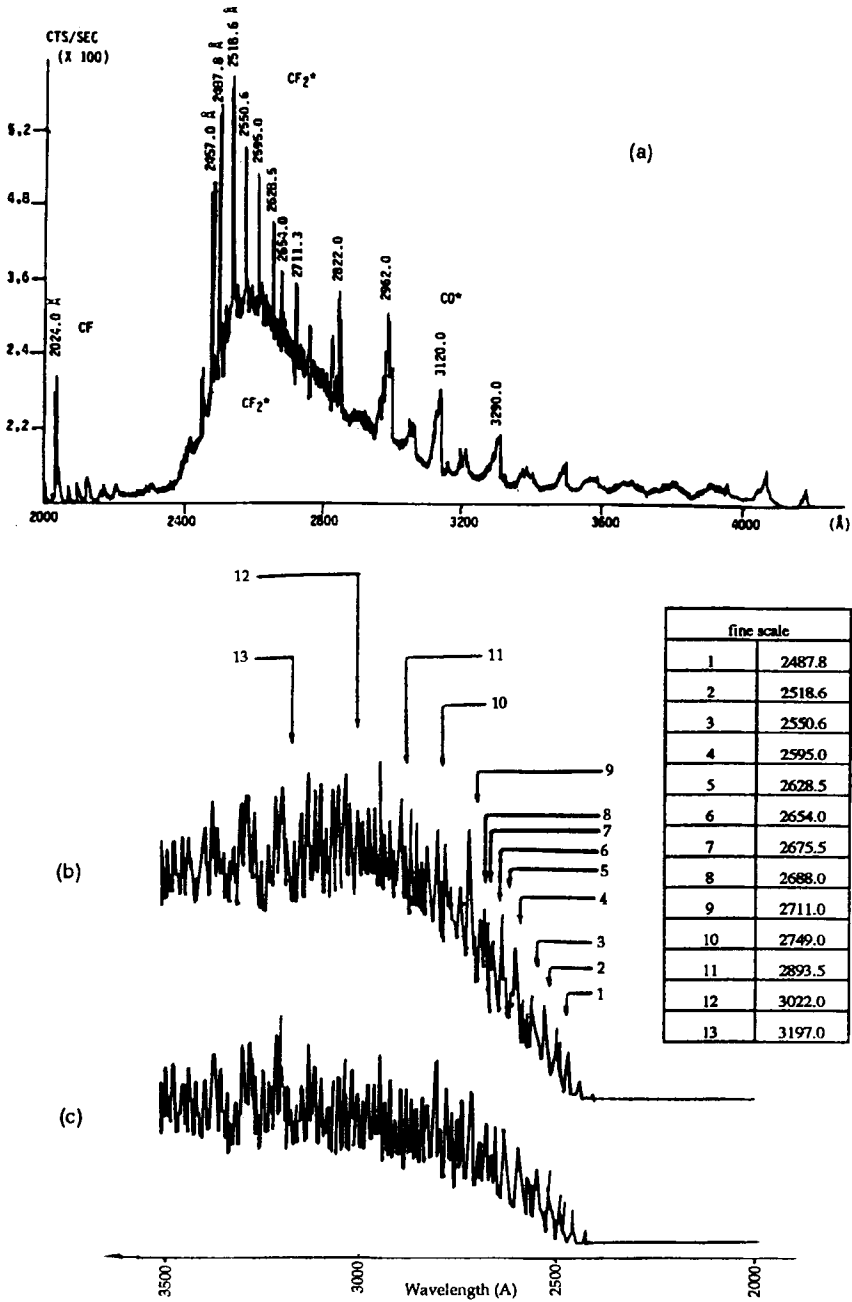
FIG. 2. Emission spectrum of CF_4 microwave plasma (a: Case E), of CF_4 Maxi-ERIS source (b: HP $= 9 \times 10^{-5}$ mbar, c: LP $= 4 \times 10^{-5}$ mbar, Cases A–D).
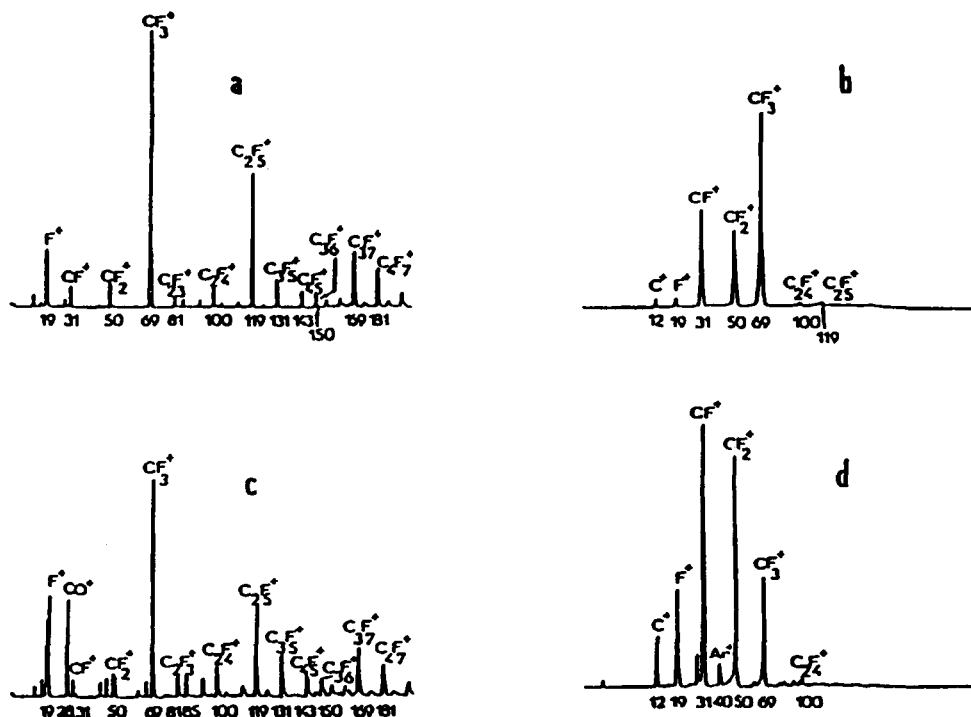
FIG. 3.   Ion beam and neutral composition for two values of the CF_4 gas flow rate as injected into the source discharge chamber. (a and b): Neutrals and ions for the resulting highest pressure HP $= 9 \times 10^{-5}$ mbar within the interaction chamber. (c and d): The corresponding spectra for the lowest pressure LP $= 4 \times 10^{-5}$ mbar. Ions and neutral species mass spectra of CF_4 Maxi-ERIS source (Cases A–D).

> On weight measurement of each sample before and after plasma treatment, representative of formation of low molecular weight products and therefore representative of degradation. If degradation takes place, thickness variation is positive; when fluorination is the most important reaction, it is negative,
>
> On surface energy that depends partially on the creation of polar or apolar groups, consequently on functionalization.

When hexatriacontane film is exposed to a Maxi-ERIS source with a high (low-pressure) or low (high-pressure) fragmentation of CF_4 gas, no important variations of sample weight are observed. If ions reach the organic target, the hexatriacontane surface becomes yellow; degradation is possible but too low to be measured. In an opposite manner, when the surface is exposed to microwave plasma, the dependence of hexatriacontane film thickness versus duration (Fig. 4) shows a low weight variation but one which is always higher than the absolute error (3×10^{-2} μm). Treatment time plays a major role in degradation; the longer it is, the higher is the degradation rate.

Surface characterization that involves a few monolayers needs specific analysis, sometimes not really well adapted to a polymer surface. Nevertheless, some of
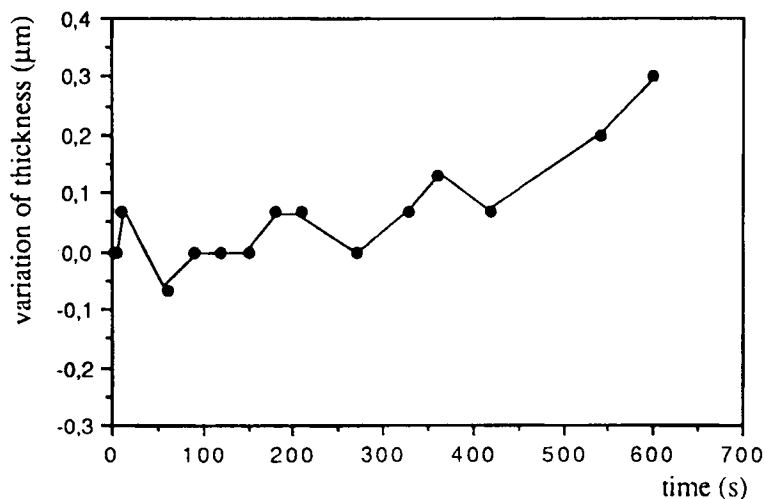
FIG. 4.   Dependence of hexatriacontane film thickness on time in microwave plasma.

them are experimentally simple, like surface energy measurement through contact angle determination with different liquids. In the case of a hexatriacontane modification study, wettability measurement is not an absolute measurement since one of the assumptions of surface energy theory ("the sample surface must be smooth, uniform and homogeneous") [31] is not really confirmed because hexatriacontane is a crystalline compound. However, the variation of surface energy should help in the interpretation of hexatriacontane modification.

The surface energies of the blank sample are $\gamma = 21.0$ mJ$\cdot$m^{-2}, $\gamma^P = 1.7$ mJ$\cdot$m^{-2}, and $\gamma^D = 19.3$ mJ$\cdot$m^{-2}, calculated from Dupré and Young relations using distilled water and diiodomethane references.

As has been described elsewhere [31, 32], interaction between CF$_4$ plasma and the hexatriacontane surface leads to a decrease of surface energy and the polar term becomes practically negligible (Fig. 5, Table 2).

Fluorination of the n-alkane in microwave plasma (Fig. 5) is complete for $t = 120$ seconds as surface energy reaches a steady state for higher irradiation: $\gamma = 3$ mJ$\cdot$m^{-2}. So a low surface energy probably means surface degradation and the appearance of fluorinated oligomers as described in Reference 9. As mentioned before, for longer exposure, degradation becomes important.

Interactions with reactive fluorinated species coming from the Maxi-ERIS source and the n-alkane surface seem to be weaker than in microwave plasma. A minimum is reached at $t = 5$ minutes, and then the global and polar energies are increased again; this increase could be interpreted as degradation dominating the fluorination mechanisms. Whatever the fragmentation level or the electron addition to CF$_4$ flux, the global surface energy decreases to reach a minimum at $t = 300$ seconds, probably due to the lack of precision in contact angle measurements.

Chemical Structure of Modified Hexatriacontane Surface

The morphology of the hexatriacontane surface has been studied by SEM (Figs. 6a and 6b). Blank sample photography shows a surface composed of a lamella
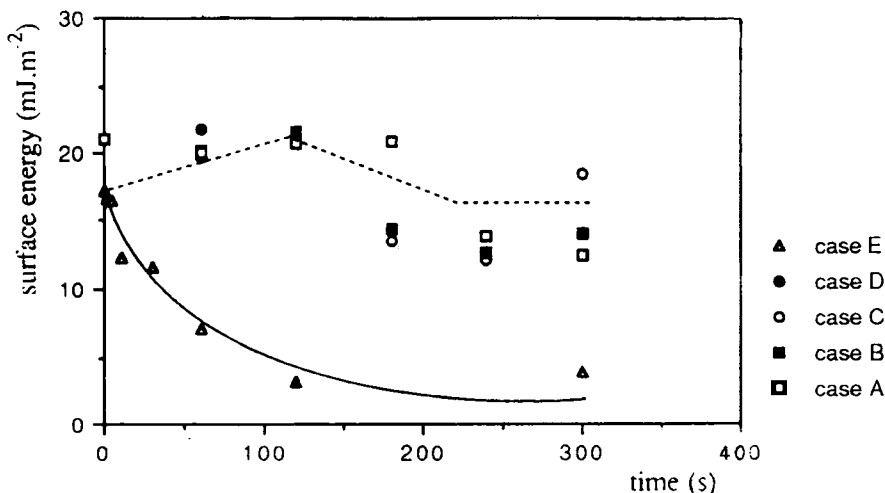
FIG. 5.   Dependence of surface energy of hexatriacontane film on time (Cases A–E).
(The dashed line is an illustration of surface energy variation.)

superposition corresponding to hexatriacontane crystals. The white cross is the
beginning point of crystal growth. CF_4 microwave plasma treatment affects the
surface topology of hexatriacontane film; the crystal microdomains disappear and
surface is flatter.

FT-IR-ATR analysis, even if it is not a real surface analysis technique, should
help in giving evidence of fluorination [32]. The transmission spectra of hexatria-
contane and a commercial polytetrafluoroethylene (Teflon) (Fig. 7a) indicate that if
hexatriacone fluorination takes place, it should lead to new strong vibrations bonds
around 1200–1000 cm^{-1}, corresponding to CF_x $(x = 1, 2)$ groups.

Effectively, ATR spectra of modified hexatriacontane show new absorption
bonds (Fig. 7b) at 1248–1226 cm^{-1} for CF_2 and CF, and at 1148 cm^{-1} for CF. The
area of these bonds increases with increasing time of irradiation.

The ATR spectra of samples treated in any Maxi-ERIS source configuration
are similar to the blank one, meaning that there is either no fluorination, or fluori-
nation of the surface on a few layers that cannot be detected with this technique, or
no grafting of reactive fluorinated species; only adsorption of the reactive fluori-
nated species takes place.

From an ESCA analysis interpretation (Fig. 8, Table 3), it is concluded that
fluorine is detected at the sample surface in any case. However, atomic fluorine
concentration seems to depend more on electron addition than on fragmentation
(high or low pressure) during Maxi-ERIS treatment. It reaches 40% for 20% with-
out electron flux, but that is lower than in a microwave treatment (53%) and in a
remote position (Case F, 58%). The oxygen observed with Maxi-ERIS and CF_4
plasma in Case G should probably be attributed to in-situ contamination.

The load effect is around 3.5 eV, as for many organic materials.

Deconvolution of the C_{1s} peak shows a shoulder at higher bond energies,
which indicates the presence of more electronegative groups than methylene groups.

TABLE 2. Values of Different Surface Energies (Cases A–E)

t (s)	Case A γ^P	Case A γ^D	Case B γ^P	Case B γ^D	Case C γ^P	Case C γ^D	Case D γ^P	Case D γ^D	Case E γ^P	Case E γ^D
2									2.77	12.38
5									1.03	13.01
10									0.23	8.81
30									0.14	8.29
60	0.53	19.47	1.96	18.19	1.86	17.83	1.84	19.83	1.24	4.04
90									0.33	4.05
120	0.26	20.57	0.61	21.45	1.06	19.82	1.07	20.18	0.01	7.40
150									0.09	2.71
180	0.25	20.56	0.30	14.04	0.64	12.86	0.64	12.86	0.52	0.84
210									0.83	1.93
240	0.83	13.03	0.30	12.35	0.67	11.52	0.64	11.52	0.21	1.41
270									0.56	0.84
300	0.50	12.47	0.00	14.04	0.38	18.01	1.38	17.01	0.16	3.66
330									0.004	2.10
360									0.16	1.92
420									0.30	3.32
480									0.24	1.97
540									0.73	2.52
600	0.87	16.90			0.93	17.49			0.59	1.29
900	1.37	21.22			1.03	15.94				
1800	1.74	21.77			1.52	21.69				
3600	2.19	26.02			1.79	21.13				

Except for microwave treatment that leads to a certain selectivity in chemical composition, CF_2 groups are prevalent, especially in a remote plasma (Case F); the other treatments lead to a surface grafted with CF, CF_2, and CF_3 groups in equal relative concentrations. Selectivity of the plasma phase (high fragmentation: CF* ions and radicals are prevalent; low fragmentation: CF$_3^*$ is the major product) does not occur on the hexatriacontane surface.

Another shoulder at 284 eV is interpreted as indicating the presence of a graphite, perhaps tetravalent carbon graphite.

Global compositions of fluorine and carbon can be calculated from the ratio of their respective atomic concentrations:

$$X = \frac{[F]}{[C]} = \frac{[F_{1s}]}{[C_{1s}]}$$

From C_{1s} deconvolution, the relative concentration of fluorine chemically bound to carbon can be determined as described in Reference 33:

$$R = \frac{[F_{C_{1s}}]}{[C]} = \frac{\displaystyle\sum_x xI_{CF_x}}{I_{C_{1s}}}$$
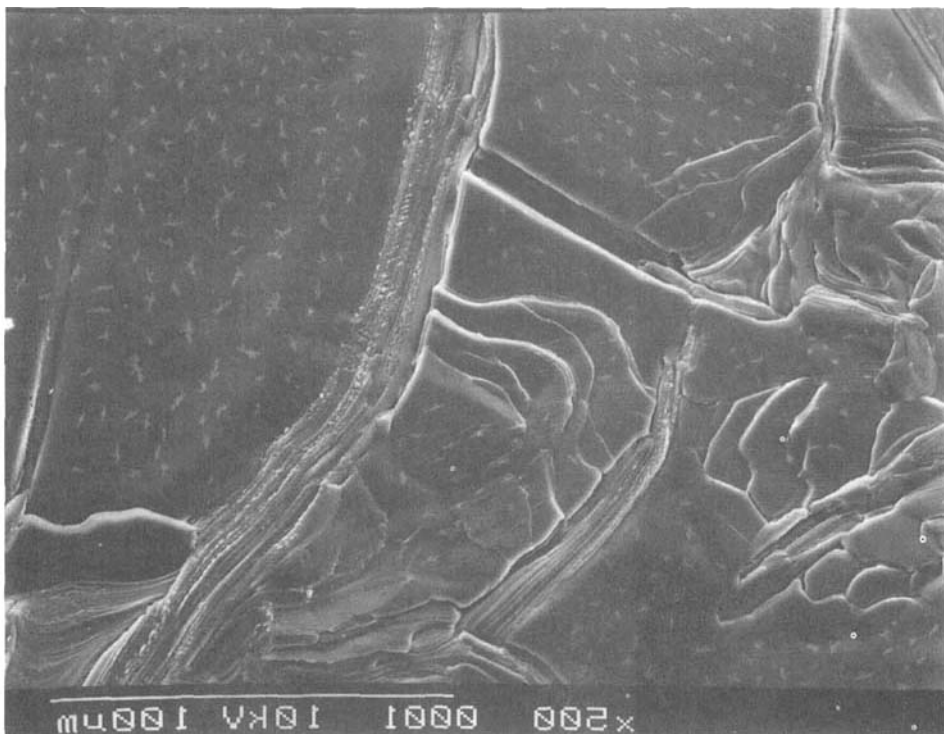
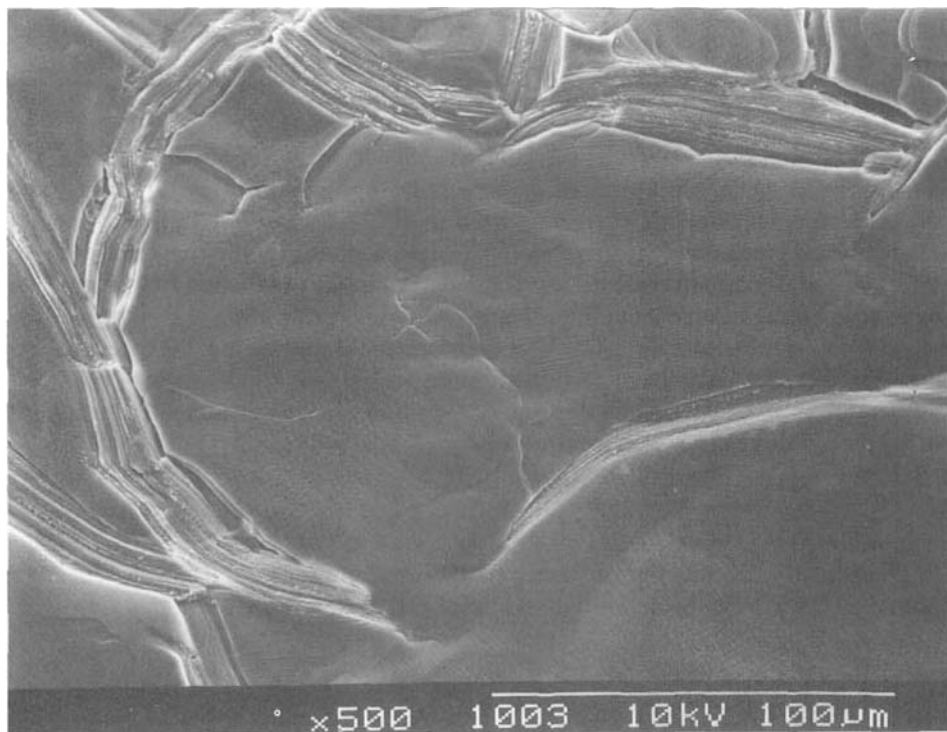FIG. 6a.   SEM of untreated hexatriacontane film in microwave plasma.

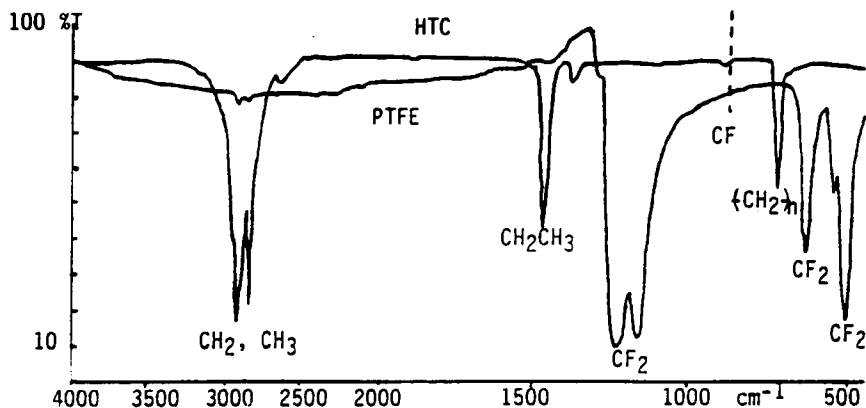FIG. 6b.   SEM of treated hexatriacontane film in microwave plasma.

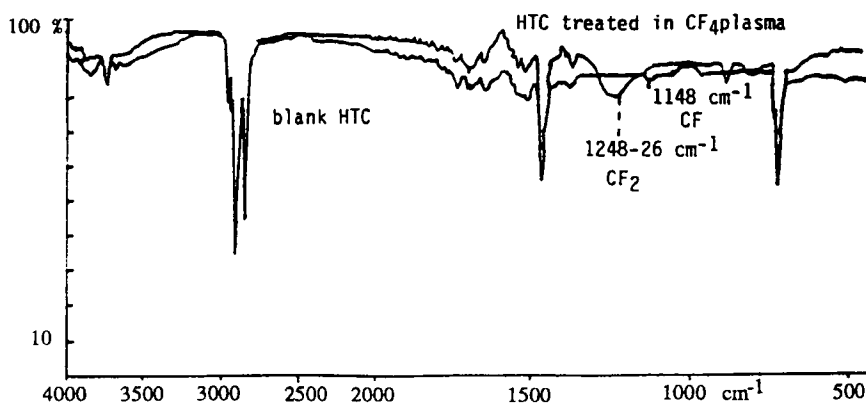FIG. 7a. Transmission spectra of hexatriacontane and fluorinated polymers.

FIG. 7b. ATR spectra of hexatriacontane and fluorinated polymers.

where $x = 1$ to 3

I_{CF_x} = intensity of CF_x groups contribution in C_{1s} peak

$I_{C_{1s}}$ = total intensity of C_{1s} peak

When electrons reach the target or when hexatriacontane is treated in microwave plasma, or not too far from its edge (Case F), the [F]/[C] and $[F_{C_{1s}}]$/[C] ratios are similar (Table 3), leading to the conclusion that all fluorine atoms present on the surface are chemically grafted on carbon atoms. In this case the fluorination could oppose the electron-assisted polymerization of CF_n^* radicals, as already described [34]. In an opposite manner, without electron flux or in remote plasma (Case G), the $[F_{C_{1s}}]$/[C] ratio is weaker:

0.08 instead of 0.33 for [F]/[C]

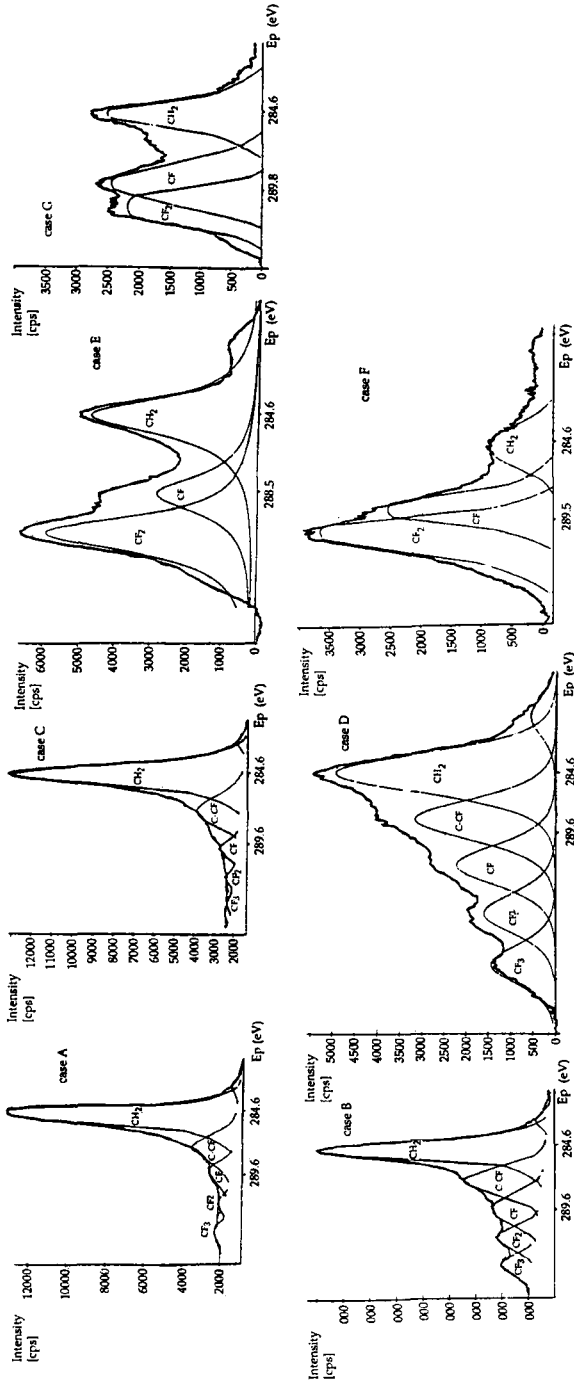0.14 instead of 0.26 for [F]/[C]

0.94 instead of 1.46 for [F]/[C]

FIG. 8. ESCA spectra of untreated or treated hexatriacontane (Cases A–G).

TABLE 3. Relative Concentrations of Different Elements and of Fluorinated Groups[a]

	F	C	O	I_{CF}	I_{CF_2}	I_{CF_3}	R	X	Δ	l
Case A	19	72	9	6	1	2	0.14	0.26	2.6	1.13
Case B	37	58	5	15	9	7	0.54	0.64	2.5	1.57
Case C	23	69	8	3	1	1	0.08	0.33	2.6	1.20
Case D	37	58	5	16	11	10	0.68	0.64	2.5	2.02
Case E	53	47	0	22	43	—	1.08	1.13	2.1	1.61
Case F	58	42	0	33	49	—	1.31	1.38	2.5	—
Case G	51	35	14	—	—	—	—	—	—	—

[a]Cases A–D, $t = 3$ minutes; Cases E and F, $t = 1$ minute; Case G, $t = 5$ minutes. Δ: FWHM (full width of half maximum), eV. l: thickness of fluorinated layer, nm.

In Case G, This difference between the two ratios must be larger than they have been calculated with oxygen present and interference in the C_{1s} peak.

In these examples, only 20% (Case C), 47% (Case A , Cases F and G) of fluorine atoms are bound to carbon atoms, the others should be only adsorbed. The treatment with Maxi-ERIS source without electrons and remote plasma treatment lead rather to fluorine atom absorption than fluorine grafting. The fluorine atoms peak, when sample is treated without electrons, is broad, this width is representative of two kinds of fluorine atoms.

The thickness of the fluorinated layer (l) can be calculated from the relation [33]

$$l = D_{C_{1s}} \ln \left(\frac{I_{C_{1s}}\text{blank}}{I_{C_{1s}}\text{treated}} \right)$$

with $D_{C_{1s}} = 1.6$ nm attenuation length.

As noticed before, treatments in microwave plasma or with a Maxi-ERIS source and electrons lead to a fluorinated layer of 1.6 to 2 nm instead of 1.1–1.2 nm as with the other treatments.

The difference between grafted fluorinated layers at the hexatriacontane surface in high- or low-pressure systems without electrons (Cases A and C) can be explained by the difference of the CF_x radical concentration in the plasma phase. A higher radical concentration is assumed at high pressure compared to low pressure, and consequently leads to a higher grafting rate at the hexatriacontane surface.

CONCLUSION

In this paper, the surface modification of a model molecule of high density polyethylene:hexatriacontane by tetrafluoromethane microwave plasma and by reactive fluorinated species bombardment is described:

1. The plasma species lead to the appearance of new chemical groups, CF_x, with CF_2 as the prevalent product.
2. Radical flux should entail only fluorine atom absorption.

We have also noticed that ion bombardment in synergy with reactive species seems to involve etching of the substrate. More studies must be done on the interactions of these different species with model surfaces.

ACKNOWLEDGMENTS

REFERENCES

[1]   H. Gleich, R. M. Criens, H. G. Moslé, and U. Leute, *Int. J. Adhes. Adhes.*, *9*(2), 88 (1989).

[2]   R. M. Podhajny, *J. Plast. Film Sheet.*, *4*, 177 (1987).

[3]   T. Yasuda, T. Okuno, and K. Yoshida, *J. Polym. Sci., Polym. Phys. Ed.*, *26*, 1781 (1988).

[4]   F. Clouet, F. Epaillard, and Y. Segui in *Interactions Plasmas froids-Matériaux* (C. Lejeune, Ed.), Editions de la Physique, Paris, 1988, p. 429.

[5]   D. T. Clark and L. Wilson, *J. Polym. Sci., Polym. Chem. Ed.*, *21*, 837 (1983).

[6]   R. Claude, M. Moisan, M. R. Wertheimer, and Z. Zakrzewski, *Polym. Mater. Sci. Eng.*, *56*, 134 (1987).

[7]   G. A. Corbin, R. E. Cohen, and R. F. Baddour, *Macromolecules*, *18*, 98 (1985).

[8]   G. A. Corbin, R. E. Cohen, and R. F. Baddour, *J. Appl. Polym. Sci.*, *30*, 1407 (1985).

[9]   D. T. Clark, W. J. Feast, W. K. R. Musgrave, and I. Ritchie, *J. Polym. Sci., Polym. Chem. Ed.*, *13*, 857 (1975).

[10] F. Poncin-Epaillard, B. Pomepui, and J. C. Brosse, *Ibid.*, *31*(11), 2671 (1993).

[11] F. Poncin-Epaillard, G. Legeay, and J. C. Brosse, *J. Appl. Polym. Sci.*, *44*, 1513 (1992).

[12] F. Normand, A. Granier, F. Clouet, Y. Holl, and M. K. Shi, *Le Vide, Les Couches Minces*, *256*, 359 (1991).

[13] F. Clouet and Y. Holl, *Ibid.*, *256*, 250 (1991).

[14] M. K. Shi, Y. Holl, Y. Guilbert, and F. Clouet, *Makromol. Chem., Rapid Commun.*, *12*, 277 (1991).

[15] F. Poncin-Epaillard, C. Lejeune, and I. Rouger, *Le Vide, Les Couches Minces*, *256*, 253 (1991).

[16] C. Lejeune, *C. R. Acad. Sci. Paris*, *296*, 1381 (1983).

[17] C. Lejeune and G. Gautherin, *Vacuum*, *34*(1-2), 251 (1984).

[18] C. Lejeune and J. P. Grandchamp, *8th International Conference IPAT Bruxelles, Symp. Proc.*, 1991, p. 356.

[19]   E. Collard, C. Lejeune, J. P. Grandchamp, P. Scheiblin, and J. P. Gilles, *Thin Solid Films*, *193*, 100 (1990).

[20]   I. Rouger, J. P. Grandchamp, M. Hamedi, and C. Lejeune, *8th International Conference IPAT, Bruxelles, Symp. Proc.*, 1991, p. 24.

[21]   F. Poncin-Epaillard and J. C. Brosse, *Makromol. Chem.*, *191*, 691 (1990).

[22]   F. Poncin-Epaillard, B. Chevet, and J. C. Brosse, *Eur. Polym. J.*, *26*(3), 333 (1990).

[23]   F. Poncin-Epaillard, B. Chevet, and J. C. Brosse, *Makromol. Chem.*, *192*, 1589 (1991).

[24]   F. Clouet, F. Massines, L. Fourmeaux, D. Mary, and F. Poncin-Epaillard, *Le Vide, Les Couches Minces*, *256*, 362 (1991).

[25]   A. Dupré, *Théorie Mécanique de la Chaleur*, Gauthier-Villars, Paris, 1969.

[26]   P. Montazer-Rahmati, F. Arefi, J. Amouroux, and A. Ricard, *Proc. 9th ISPC*, 1989, p. 1195.

[27]   J. Bretagne, F. Epaillard, and A. Ricard, *J. Polym. Sci., Polym. Chem. Ed.*, *30*, 323 (1991).

[28]   R. D'Agostino, F. Cramarossa, and S. de Benedictis, *Plasma Chem. Plasma Proc.*, *2*(3), 213 (1982).

[29]   S. Mournet, F. Arefi, M. Goldman, and J. Amouroux, *Proc. 9th ISPC*, 1989, p. 1167.

[30]   E. Kay, J. Corbun, and A. Dilks, *Top. Curr. Chem.*, *94*, 1 (1980).

[31]   J. D. Andrade, L. M. Smith, and D. E. Gregonis, in *Surface and Interfacial Aspects of Biomedical Polymers*, Vol. 1 (J. D. Andrade, Ed.), Plenum, New York, 1985, p. 249.

[32]   F. Poncin-Epaillard and J. C. Brosse, *Makromol. Chem.*, *191*, 1451 (1990).

[33]   E. Collard, *Thèse*, Orsay, June 1990.

[34]   I. Rouger, J. P. Grandchamp, M. Hamedi, and C. Lejeune, *1st European Workshop on Plasma Ion Surface Engineering, Symp. Proc.*, 1991.